bnhcrc.com.au

# MODEL FOR ASSESING THE VULNERABILITY OF AUSTRALIAN HOUSING TO WINDSTORMS - VAWS

**Korah Parackal[1], Martin Wehner[2], Hyeuk Ryu[2], John Ginger[1], David Henderson[1], Mark Edwards[2]**

[1]James Cook University Cyclone Testing Station, [2]Geoscience Australia & Bushfire and Natural Hazards CRC

| Version | Release history | Date |
|---|---|---|
| 1.0 | Initial release of document | 19/12/2019 |

Australian Government
Department of Industry, Innovation and Science

Business
Cooperative Research
Centres Programme

**Publisher:**
Bushfire and Natural Hazards CRC

December 2019

Citation: Parackal, K, Wehner, M, Ryu, H, Ginger, J, Henderson, D, Edwards M 2019 'Improving the resilience of existing housing to severe wind events', Annual Report, Bushfire and Natural Hazards CRC, Melbourne 2019.

Cover: Damage to houses in northern Queensland from 2009 cyclone.

## TABLE OF CONTENTS

# 1 INTRODUCTION

Modelling the vulnerability of houses in windstorms is important for insurance pricing, policy-making, and emergency management. Models for Australian house types have been developed since the 1970s, and have ranged from empirical models to more advanced reliability based structural engineering models, which provide estimates of damage for a range of wind speeds of interest. This report describes the development of a software program: Vulnerability and Adaption to Wind Simulation (VAWS), which uses probability based reliability analysis and structural engineering for the loading and response coupled with an extensive test database and field damage assessments to calculate the damage experienced by selected Australian house types.

VAWS consists of probabilistic modules for the 1. wind hazard – external and internal pressures generated by the atmospheric wind and 2. structural response – related to the structural system and capacities of the components and connections and load effects. The program is able to accommodate a range of house types for which the structural system and their strengths and the external pressure distribution for wind exposure from directions around the compass.

The critical structural components are probabilistically assigned their strengths and the wind loads are applied for winds approaching from a specified direction. Failure is initiated when the load exceeds the capacity of a critical component or connection as the wind loads are increased with increasing discrete wind speed increments. When components fail, loads are redistributed through the structural system. The cost of repair is calculated for the given level of damage and the damage index is calculated at each wind speed increment.

This report describes the logic of VAWS including the main modules: the house type and structural system, external and internal pressure distribution, structural response, initiation and progression of damage, windborne debris impact, water ingress and cost of repair. A case study is presented to show the preliminary outputs of VAWS for a highset Queensland house type.

# 2 OVERALL LOGIC

Vulnerability and Adaptation to Wind Simulation (VAWS) is a software package that can be used to model the vulnerability of small buildings such as domestic houses and light industrial sheds to wind (GeoscienceAustralia 2019). The primary aim of VAWS is the examination of the change in vulnerability afforded by mitigation measures to improve a building's resilience to wind hazard. The program is built around the following high level sequence as shown in Figure 1

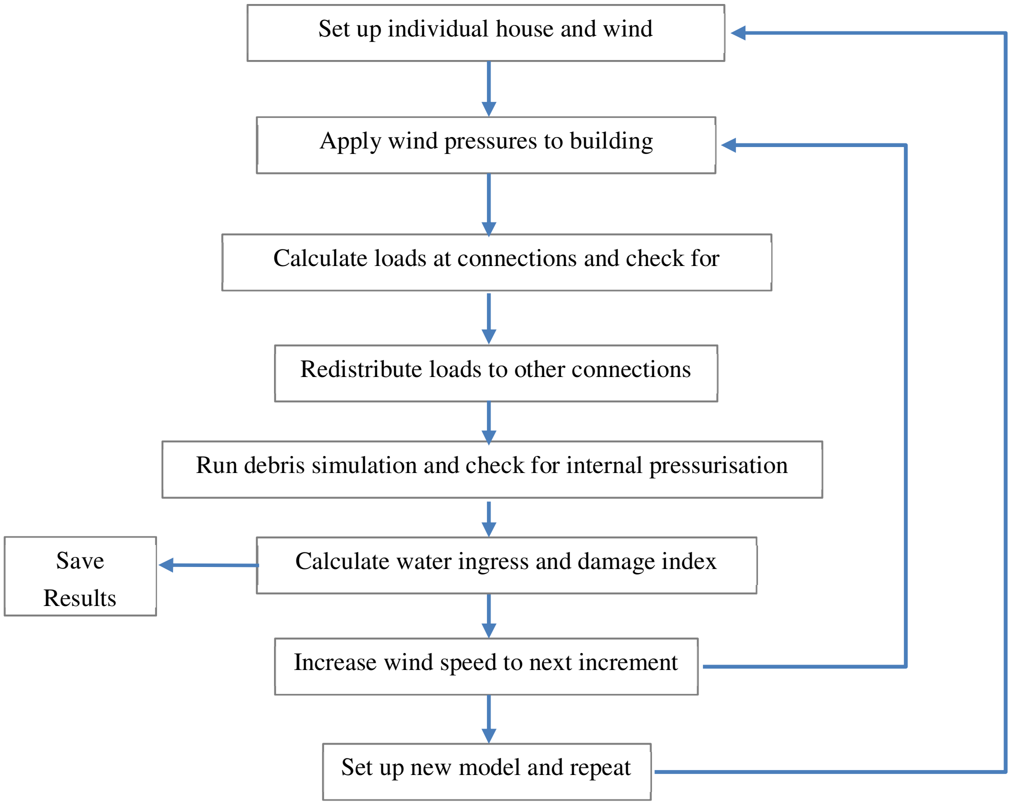

FIGURE 1 VULNERABILITY AND ADAPTION TO WIND SIMULATION (VAWS) MODEL LOGIC

The VAWS program takes a component-based approach to modelling building vulnerability. It is based on the premise that overall building damage is strongly related to the failure of key connections. The program generates a building model by selecting parameter values from predetermined probability distributions using a Monte Carlo process. Values include component and connection strengths, external pressure coefficients, shielding coefficients, wind speed profile with height, building orientation, debris damage parameters, and component masses. Then, for increasing gust wind speed increments, it calculates the forces in all critical connections using influence coefficients, assesses which connections have failed and translates these into a damage scenario and costs the repair. Using the repair cost and the full replacement cost, it calculates a damage index for each wind speed.

## KEY PARAMETERS AND VARIABILITY

The Monte Carlo process captures a range of variability in both wind loading and component parameters. The parameter values are sampled for each realisation of the modelled house and kept the same as the wind speed is incremented up to a set maximum.

- Wind direction

  For each house, its orientation with respect to the wind is chosen from the eight cardinal directions either randomly, or set constant by the user.

- Gust wind profile

  Variation in the profile of wind speed with height is captured by the random sampling of a profile from a suite of user-provided profiles.

- External pressure coefficients for zones and coverages

  External pressure coefficients for different zones of the house surfaces envelope are randomly chosen from a Type III (Weibull) extreme value distribution with specified means and coefficients of variation for different zones of the house envelope.

- Construction level (or quality)

  construction quality can be defined with mean and coefficient of variation (CV) factors which are used to adjust the mean and CV of distribution of connection strength.

- Strength and dead load

  Connection strengths and dead loads for generated houses are sampled from lognormal probability distributions specified by the user.

# 3 SIMULATION MODULES

The VAWS program consists of several modules that simulate the behaviour described in the overall program logic.

## APPROACH WIND PROFILES

Boundary layer profiles of wind velocity for several terrain categories are defined according to (JDHConsulting 2010)

## EXTERNAL PRESSURE COEFFICIENTS

The Building envelope is divided into zones corresponding to the framing plan of the house e.g. at batten to rafter intersections and wall stud locations. External wind pressures on these zones are determined from wind tunnel model testing. The average of the minimum peak pressure coefficients within a 45 degree wind approach sector was used to derive the pressure distributions used for 8 cardinal directions.

These wind tunnel derived pressures account for local pressure effects in flow separation regions and can be used for the application of load to cladding and immediate supporting members such as batten to rafter connections. The pressures are factored by 0.7 for load application to major structural elements to account for area averaging effects of pressure fluctuations of real wind loads.

## INTERNAL PRESSURE COEFFICIENTS

Internal pressure coefficients are calculated following the logic contained in the wind loading standard AS/NZS 1170.2 depending on the distribution and sizes of openings in the walls. The presence of openings is determined by modelling debris impact during a storm and pressure-induced failures of windows and doors.

The internal pressure in the nominally sealed house with the envelope intact (ie doors and windows shut) is small Cpi = 0. However the failure of a door or window on the windward wall from wind pressure or debris impact with increasing wind speed will result in the internal pressure reaching the values of the external wall pressure at the dominant opening Cpi = 0.6 or more.

## WINDBORNE DEBRIS

Internal pressurisation due to debris impact on windows and doors can cause large increases in uplift forces. Modelling the generation, trajectories and impact of debris is a complex process and VAWS contains a dedicated module based on work by Wehner, Sandland et al. (2010)

## STRUCTURAL RESPONSE AND LOAD REDISTRIBUTION

The VAWS program accounts for load redistribution and progressive failures of the roof without the use of computationally intensive non-linear structural analysis by incorporating several simplifying assumptions. Connection considered in the analysis include: cladding fasteners, batten to rafter connections and rafter to top plate connections. The program relates pressures applied to envelope zones to the cladding connection loads and the supporting structure using linear elastic influence coefficients. Once connections have failed, the effects of redistribution are preserved for successive wind speed increments, thus ensuring that increasing wind loads act on the damaged structure rather than beginning anew with an intact structure. Following connection failures, redistribution of loads is modelled by changing the values of influence coefficients depending on the positon of the failed connection in the load path.

## CONNECTION STRENGTHS

Connection strengths are derived from engineering judgement and testing conducted at the Cyclone Testing Station. Some strengths are modified to account for fatigue and load sharing effects. Strengths are assigned to connections in the VAWS model by sampling log normal probability distribution functions.

## INFLUENCE COEFFICIENTS

A large data base of influence coefficients is provided as input data for an intact house. The influence coefficients are determined from a finite element structural analysis model or full scale testing.

A second large database of influence coefficients is provided that describe the changes in load path that occur after failure of connections in the roof structure, i.e. connections below the batten to rafter connections such as rafter to top plate or collar tie to rafter, etc. For each roof structure connection, new influence coefficients are provided for each roof structure connection on the rafter line of the failed connection and the rafter line immediately adjacent. Each roof structure connection would typically have an influence coefficient relating the force in the connection to the force in each batten to rafter connection on its rafter line.

## WATER INGRESS

Water ingress is estimated in order to account for the large costs associated with water damage to internal linings. Predefined relationships for water damage as a function of wind speed are selected based on the extent of damage to the house envelope, shown in Figure 2.

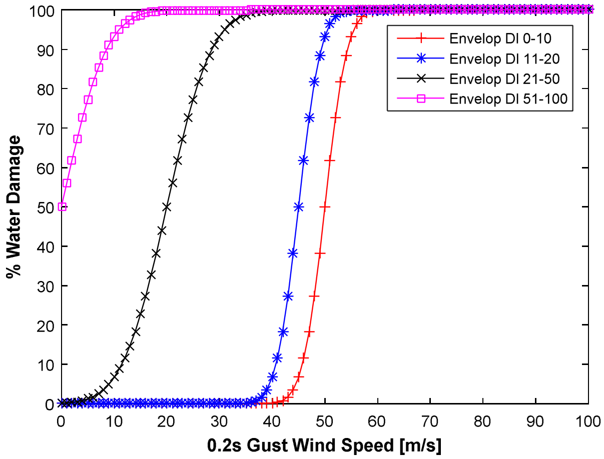

FIGURE 2. WATER INGRESS FOR DIFFERENT LEVELS OF BUILDING ENVELOPE DAMAGE WITH VARYING WINS SPEED

## DAMAGE COSTING

The program determines a repair cost for a damaged house by modelling the damage state(s) which a house is in at each wind speed and then costing the required repair work. The modelled house may have experienced one or more damage states (for example, *Loss of Roof Sheeting* and *Debris Damage to Walls*). The repair cost for any particular damage state is made up of two components: repair to damage to the external envelope and repair of consequential damage to the interior with repair of interior damage caused by water ingress calculated separately. Thus, the total repair cost for a house type at a wind speed is expressed as:

$$Total\ repair\ cost = \left( \sum_{All\ damage\ states\ i} External\ envelope\ repair\ cost_i + Consequential\ internal\ repair\ cost_i \right) + Water\ ingress\ repair\ cost$$

The two components of the repair cost for each damage state $i$ are calculated as below. The calculation allows for each damage state to only affect part of the total susceptible area (for example, only a corner of the roof may have lost its roof sheeting).

$$External\ envelope\ repair\ cost_i = Total\ quantity_i \times Percent\ damage_i \times Repair\ rate_i \times f_i(Percent\ damage)$$

$$Consequential\ internal\ repair\ cost_i = Internal\ repair\ cost_i \times Percent\ damage_i \times f_i(Percent\ damage)$$

Where $f_i(Percent\ damage)$ are functions adjusting the repair rate to allow for higher repair rates for extents of repair less than full repair. It is in the form of a quadratic equation $(a_1x^2 + a_2x + a_3)$ where $x$ is the percent damage in a particular damage state and $a_1$ to $a_3$ are supplied coefficients.

The repair cost due to water ingress is calculated from the modelled degree of water ingress, the dominant damage state and repair costs supplied in the costing data as follows.

$$Water\ ingress\ repair\ cost_i = Water\ ingress\ repair\ cost_{i,\%} \times f_i(Percent\ damage)$$

Where $Water\ ingress\ repair\ cost_{i,\%}$ is repair cost data supplied as part of the costing module for repair of damage caused by water ingress for a house.

The costing algorithm contains logic to prevent double counting of repair to building components where component repair is nominated in multiple damage states.

The project expresses repair costs as a damage index (DI) calculated as:

$$Damage\ Index = \frac{Total\ building\ repair\ cost}{Building\ replacement\ cost}$$

This permits the results to be applied to other houses of similar generic type but different floor areas. The repair cost is then calculated by multiplying the DI by the floor area and the replacement rate for the generic house type.

# 4 CASE STUDY – VULNERABILITY OF A HIGH-SET QUEENSLAND HOUSE

## THE GROUP 4 HOUSE:

The VAWS software was used to model the vulnerability of a highset Queensland house. The model details and an interpretation of the results is presented in the following sections.

The house is a high set timber framed structure with metal roof cladding and fibre cement wall cladding, an example shown in Figure 3. The dimensions and structural system were determined from survey data and the resulting representative house was originally described in Henderson and Harper (2003). It is known as the Group 4 House.

The house is 12.6 m long, 7.3m wide and 4.4 m tall including 2.0m stumps. The roof structure consists of rafters at 10 degree pitch at 900 c/c supporting battens at 900cc that in turn support corrugated metal cladding. The overall dimensions and locations of windows and doors are shown in Figure 4. A schematic of the roof structure and a framing plan showing the locations of battens and rafters is shown in Figure 5.

### Assumptions

This case study focuses on the modelling of structural damage to the roof of a population of Group 4 houses. In order for the damage index to represent the cost of repair of structural damage, certain settings are implemented to ensure the extent of damage is calculated based on structural damage alone:

- Water ingress is turned off to allow the damage index to be based on structural damage only
- Debris damage is not costed (by setting the repair rate to zero) so that the damage index is excludes the cost of repair of wall cladding but allows for the effects of internal pressures.
- Failure of windows, etc. by wind pressure is suppressed (by making the component strengths very large) such that internal pressurisation only occurs due to debris impact.

FIGURE 3 EXAMPLE OF A GROUP 4 HOUSE TYPE

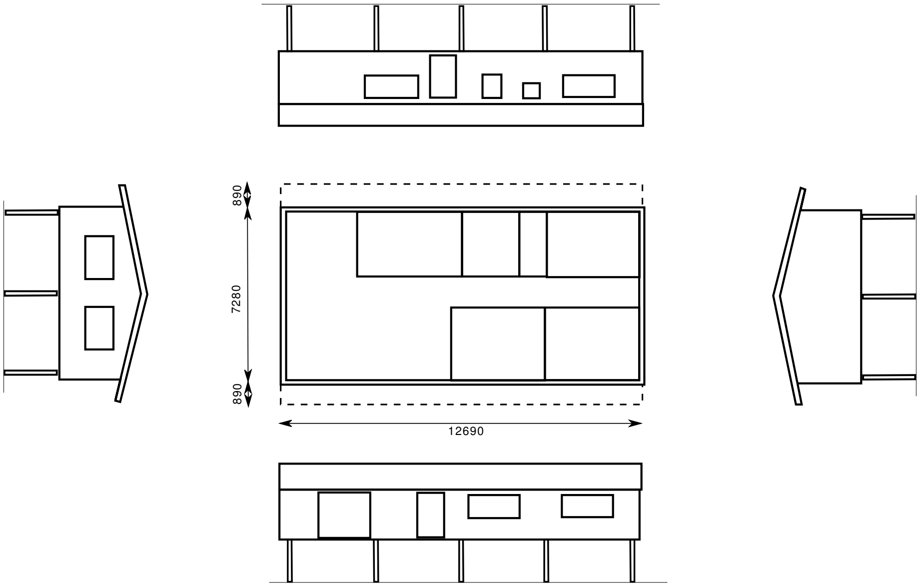

FIGURE 4 DIAGRAM OF GROUP 4 HOUSE

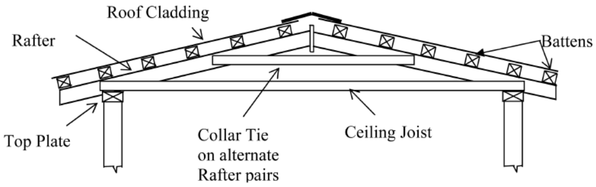

FIGURE 5 ROOF STRUCTURE OF THE GROUP 4 HOUSE

## INPUTS:

### Wind pressures

Wind loads on the Group 4 House are determined by carrying out a wind tunnel model study. The model used was originally tested by Holmes and Best (1978) and has similar dimensions to the Group 4 House. The model was modified to reduce to size of the eaves to be more representative of the Group 4 House.

The tests were carried out in the 2.0 m high × 2.5 m wide × 22 m long Boundary Layer Wind Tunnel at the CTS, James Cook University. The approach Atmospheric Boundary Layer profile (suburban terrain, category 2.5 as per AS/NZS1170.2) was simulated at a length scale of 1/50 using a 250 mm high trip board at the upstream end followed by an array of blocks on the tunnel floor.

Pressure taps were installed on the roof, wall and the floor of the model to measure the external pressures. Each pressure tap was connected to transducers located below the wind tunnel floor/turntable via a length of tuned PVC tubing.

External pressures on the roof, walls and floor, were obtained for approach wind directions ($\theta$) of 0° to 360° in steps of 10°. The fluctuating pressures were low-pass filtered at 500 Hz, sampled at 1000 Hz for 30 secs (corresponding to ~ 10 min in full-scale) and recorded as *p(t)* and statistically analysed to give mean, maximum and minimum pressure coefficients referenced to the mean dynamic pressure at roof height:

$$C_{\overline{p}} = \frac{\overline{p}}{\frac{1}{2}\rho \overline{U}_h^{\,2}}, \qquad C_{\hat{p}} = \frac{\hat{p}}{\frac{1}{2}\rho \overline{U}_h^{\,2}}, \qquad C_{\breve{p}} = \frac{\breve{p}}{\frac{1}{2}\rho \overline{U}_h^{\,2}}$$

Where, $\rho$ is the density of air and $\overline{U}_h$ is the mean velocity at roof height. The mean and peak pressure distributions were used to identify regions experiencing large wind loads, and for comparisons with data given in AS/NZ1170.2. This AS/NZS 1170.2 equivalent quasi-steady aerodynamic shape factor $C_{fig} = C_{peak}/G_U^2$, where $G_U = (\hat{U}_h / \overline{U}_h)$ is the velocity gust factor. Here $\hat{U}_h$ and $\overline{U}_h$ are the 0.2 sec gust wind speed and mean wind speed respectively at roof height.

### Pressure distributions

Analysis of pressure coefficients with wind direction $\theta$, show that the windward edge of the roof experiences the largest (mean and peak) suction pressures and the (windward) wall is subjected to positive pressures.

These pressures are generally close to values given in AS/NZS1170.2. The underside of the eaves are subjected to pressures similar to that on the adjacent wall surface. Roof cladding, battens and rafters near the windward gable-end experiences the largest wind pressures.

The average of the minimum pressure coefficients within a 45 degree sector was used to derive the pressure distributions used for eight cardinal directions. The wind pressure distributions for a cornering wind sector 225 ±20° is shown in Figure 6.

These wind tunnel derived pressures account for local pressure effects in flow separation regions and can be used for the application of load to cladding and immediate supporting members such as batten to rafter connections. The pressures are factored by 0.7 for load application to major structural elements to account for area averaging effects of pressure fluctuations on the tributary area of the element.

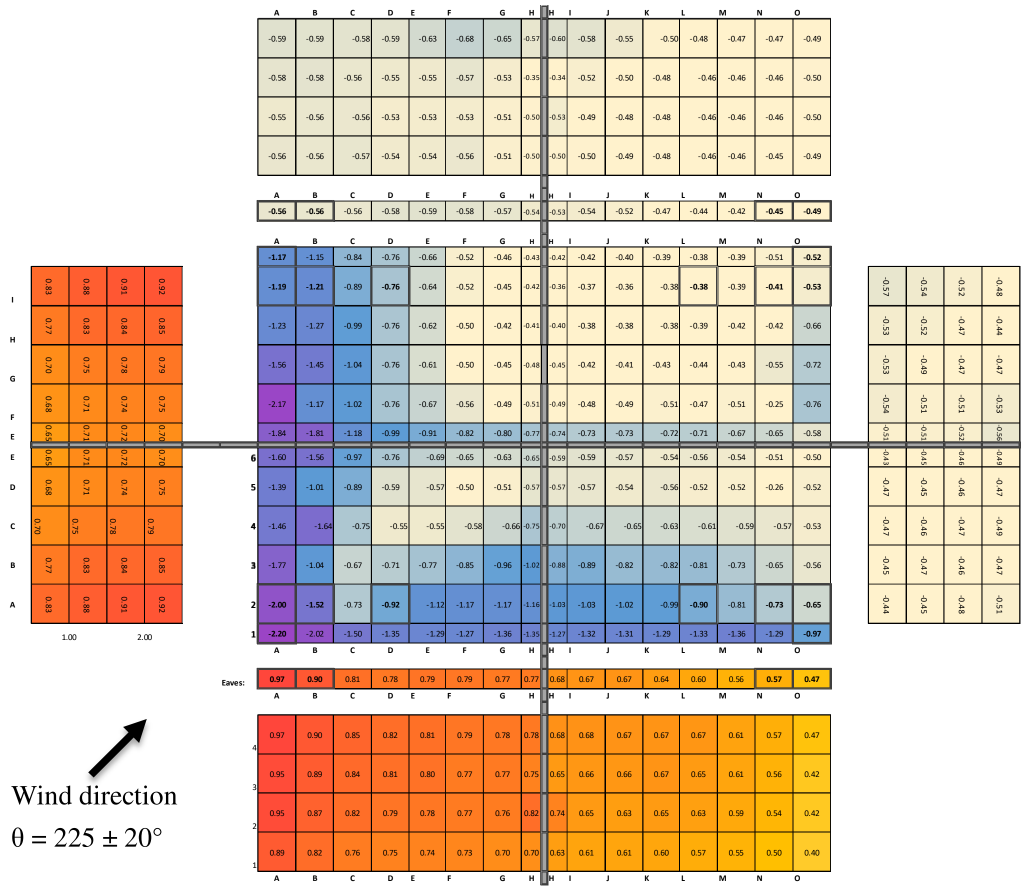

| A | B | C | D | E | F | G | H | H | I | J | K | L | M | N | O |
|---|---|---|---|---|---|---|---|---|---|---|---|---|---|---|---|
| -0.59 | -0.59 | -0.58 | -0.59 | -0.63 | -0.68 | -0.65 | -0.57 | -0.60 | -0.58 | -0.55 | -0.50 | -0.48 | -0.47 | -0.47 | -0.49 |
| -0.58 | -0.58 | -0.56 | -0.55 | -0.55 | -0.57 | -0.53 | -0.35 | -0.34 | -0.52 | -0.50 | -0.48 | -0.46 | -0.46 | -0.46 | -0.50 |
| -0.55 | -0.56 | -0.56 | -0.53 | -0.53 | -0.53 | -0.51 | -0.50 | -0.53 | -0.49 | -0.48 | -0.48 | -0.46 | -0.46 | -0.46 | -0.50 |
| -0.56 | -0.56 | -0.57 | -0.54 | -0.54 | -0.56 | -0.51 | -0.50 | -0.50 | -0.50 | -0.49 | -0.48 | -0.46 | -0.46 | -0.45 | -0.49 |

| A | B | C | D | E | F | G | H | H | I | J | K | L | M | N | O |
|---|---|---|---|---|---|---|---|---|---|---|---|---|---|---|---|
| **-0.56** | **-0.56** | -0.56 | -0.58 | -0.59 | -0.58 | -0.57 | -0.54 | -0.53 | -0.54 | -0.52 | -0.47 | -0.44 | -0.42 | **-0.45** | **-0.49** |

|  | A | B | C | D | E | F | G | H | H | I | J | K | L | M | N | O |
|---|---|---|---|---|---|---|---|---|---|---|---|---|---|---|---|---|
|  | **-1.17** | -1.15 | -0.84 | -0.76 | -0.66 | -0.52 | -0.46 | -0.43 | -0.42 | -0.42 | -0.40 | -0.39 | -0.38 | -0.39 | -0.51 | **-0.52** |
|  | **-1.19** | **-1.21** | -0.89 | **-0.76** | -0.64 | -0.52 | -0.45 | -0.42 | -0.36 | -0.37 | -0.36 | -0.38 | **-0.38** | -0.39 | **-0.41** | **-0.53** |
|  | -1.23 | -1.27 | -0.99 | -0.76 | -0.62 | -0.50 | -0.42 | -0.41 | -0.40 | -0.38 | -0.38 | -0.38 | -0.39 | -0.42 | -0.42 | -0.66 |
|  | -1.56 | -1.45 | -1.04 | -0.76 | -0.61 | -0.50 | -0.45 | -0.48 | -0.45 | -0.42 | -0.41 | -0.43 | -0.44 | -0.43 | -0.55 | -0.72 |
|  | -2.17 | -1.17 | -1.02 | -0.76 | -0.67 | -0.56 | -0.49 | -0.51 | -0.49 | -0.48 | -0.49 | -0.51 | -0.47 | -0.51 | -0.25 | -0.76 |
|  | -1.84 | -1.81 | -1.18 | -0.99 | -0.91 | -0.82 | -0.80 | -0.77 | -0.74 | -0.73 | -0.73 | -0.72 | -0.71 | -0.67 | -0.65 | -0.58 |
| 6 | -1.60 | -1.56 | -0.97 | -0.76 | -0.69 | -0.65 | -0.63 | -0.65 | -0.59 | -0.59 | -0.57 | -0.54 | -0.56 | -0.54 | -0.51 | -0.50 |
| 5 | -1.39 | -1.01 | -0.89 | -0.59 | -0.57 | -0.50 | -0.51 | -0.57 | -0.57 | -0.57 | -0.54 | -0.56 | -0.52 | -0.52 | -0.26 | -0.52 |
| 4 | -1.46 | -1.64 | -0.75 | -0.55 | -0.55 | -0.58 | -0.66 | -0.75 | -0.70 | -0.67 | -0.65 | -0.63 | -0.61 | -0.59 | -0.57 | -0.53 |
| 3 | -1.77 | -1.04 | -0.67 | -0.71 | -0.77 | -0.85 | -0.96 | -1.02 | -0.88 | -0.89 | -0.82 | -0.82 | -0.81 | -0.73 | -0.65 | -0.56 |
| 2 | **-2.00** | **-1.52** | -0.73 | **-0.92** | -1.12 | -1.17 | -1.17 | -1.16 | -1.03 | -1.03 | -1.02 | -0.99 | **-0.90** | -0.81 | **-0.73** | **-0.65** |
| 1 | **-2.20** | -2.02 | -1.50 | -1.35 | -1.29 | -1.27 | -1.36 | -1.35 | -1.27 | -1.32 | -1.31 | -1.29 | -1.33 | -1.36 | -1.29 | **-0.97** |
|  | A | B | C | D | E | F | G | H | H | I | J | K | L | M | N | O |

|  | A | B | C | D | E | F | G | H | H | I | J | K | L | M | N | O |
|---|---|---|---|---|---|---|---|---|---|---|---|---|---|---|---|---|
| Eaves: | **0.97** | **0.90** | 0.81 | 0.78 | 0.79 | 0.79 | 0.77 | 0.77 | 0.68 | 0.67 | 0.67 | 0.64 | 0.60 | 0.56 | **0.57** | **0.47** |

|  | A | B | C | D | E | F | G | H | H | I | J | K | L | M | N | O |
|---|---|---|---|---|---|---|---|---|---|---|---|---|---|---|---|---|
| 4 | 0.97 | 0.90 | 0.85 | 0.82 | 0.81 | 0.79 | 0.78 | 0.78 | 0.68 | 0.68 | 0.67 | 0.67 | 0.67 | 0.61 | 0.57 | 0.47 |
| 3 | 0.95 | 0.89 | 0.84 | 0.81 | 0.80 | 0.77 | 0.77 | 0.75 | 0.65 | 0.66 | 0.66 | 0.67 | 0.65 | 0.61 | 0.56 | 0.42 |
| 2 | 0.95 | 0.87 | 0.82 | 0.79 | 0.78 | 0.77 | 0.76 | 0.82 | 0.74 | 0.65 | 0.63 | 0.65 | 0.63 | 0.59 | 0.54 | 0.42 |
| 1 | 0.89 | 0.82 | 0.76 | 0.75 | 0.74 | 0.73 | 0.70 | 0.70 | 0.63 | 0.61 | 0.61 | 0.60 | 0.57 | 0.55 | 0.50 | 0.40 |
|  | A | B | C | D | E | F | G | H | H | I | J | K | L | M | N | O |

|  |  | 1.00 |  | 2.00 |
|---|---|---|---|---|
| I | 0.83 | 0.88 | 0.91 | 0.92 |
| H | 0.77 | 0.83 | 0.84 | 0.85 |
| G | 0.70 | 0.75 | 0.78 | 0.79 |
| F | 0.68 | 0.71 | 0.74 | 0.75 |
| E | 0.65 | 0.71 | 0.72 | 0.70 |
| E | 0.65 | 0.71 | 0.72 | 0.70 |
| D | 0.68 | 0.71 | 0.74 | 0.75 |
| C | 0.70 | 0.75 | 0.78 | 0.79 |
| B | 0.77 | 0.83 | 0.84 | 0.85 |
| A | 0.83 | 0.88 | 0.91 | 0.92 |

|  |  |  |  |
|---|---|---|---|
| -0.57 | -0.54 | -0.52 | -0.48 |
| -0.53 | -0.52 | -0.47 | -0.44 |
| -0.53 | -0.49 | -0.47 | -0.47 |
| -0.54 | -0.51 | -0.51 | -0.53 |
| -0.51 | -0.51 | -0.52 | -0.56 |
| -0.43 | -0.45 | -0.46 | -0.49 |
| -0.47 | -0.45 | -0.46 | -0.47 |
| -0.47 | -0.46 | -0.47 | -0.49 |
| -0.45 | -0.47 | -0.46 | -0.47 |
| -0.44 | -0.45 | -0.48 | -0.51 |

FIGURE 6 CFIG PRESSURE DISTRIBUTION FOR THE SECTOR 225 ±20°

## CONNECTION STRENGTHS

Connection strengths are derived from engineering judgement and testing conducted at the Cyclone Testing Station. Some strengths are modified to account for load sharing effects.

Strengths are assigned to connections in the VAWS model using log normal probability distribution functions, with the mean strengths and standard deviations shown in Table 1.

TABLE 1 CONNECTION STRENGTHS AND COMPONENT DEAD LOADS.

| Type name | Strength mean (kN) | Strength std (kN) | Dead load mean (kN) | Dead load std (kN) | Tributary area $(m^2)$ |
|---|---|---|---|---|---|
| sheeting | 2.7<br>(for approx. 4 fasteners) | 0.2 | 0 | 0 | 0.81 |
| batten | 2 | 1.3 | 0.1 | 0.1 | 0.81 |
| rafter | 10 | 5.9 | 1.7 | 0.1 | 2.46 |

## DAMAGE COSTING DATA

Cost of damage is calculated based on the number of failed connections, with each connection type corresponding to a tributary area in $m^2$ that would be affected during a failure, shown in Table 2. Cost of damage in dollars is then calculated based on the envelope repair rate shown in

Table 2. Cost of damage due to water ingress is determined by the curves shown in Figure 2. Additionally, a damage index is calculated based on the ratio of the repair cost to the cost for full replacement of the house. In this case study, the replacement cost is set to the replacement cost for the roof and associated linings and finishes such as ceilings, eave linings, cornices and painting. This ensures that damage indices will reach 1.0 for complete failure.

TABLE 2 DAMAGE COSTING COVERAGES AND UNIT COSTS

| Failure Mode | Total Surface area $[m^2]$ | Envelope repair rate $[\$/m^2]$ |
|---|---|---|
| Loss of roof sheeting | 113.4 | 72.40 |
| Loss of roof sheeting & purlins | 113.4 | 184.2 |
| Loss of roof structure | 113.4 | 317.0 |
| Wall debris damage | 135.2 | 0.000 |
| Loss of wall cladding | 106.4 | 243.7 |
| Wall collapse | 106.4 | 527.2 |
| Wall racking | 106.4 | 478.3 |
| Loss of guttering | 146 | 23.60 |

# 5 RESULTS

## RESULTS FOR A SINGLE WIND DIRECTION:

As described in previous sections, the VAWS software simulates the failure of connections and redistribution of loads to neighbouring connections in detail. Although several simplifying assumptions are involved, the vulnerability curves determined are based on structural failure behaviour that would occur during a wind storm.

Results for a single run of the wind and structure simulation for a south west wind direction are presented in this section. The external pressure distribution on the roof of the house is shown in Figure 7. Damage to the structure is presented in a series of 'heatmaps' that show the gust wind speeds at failure of for different types of connections. These diagrams indicate how loads are redistributed and how damage spreads through the structure.

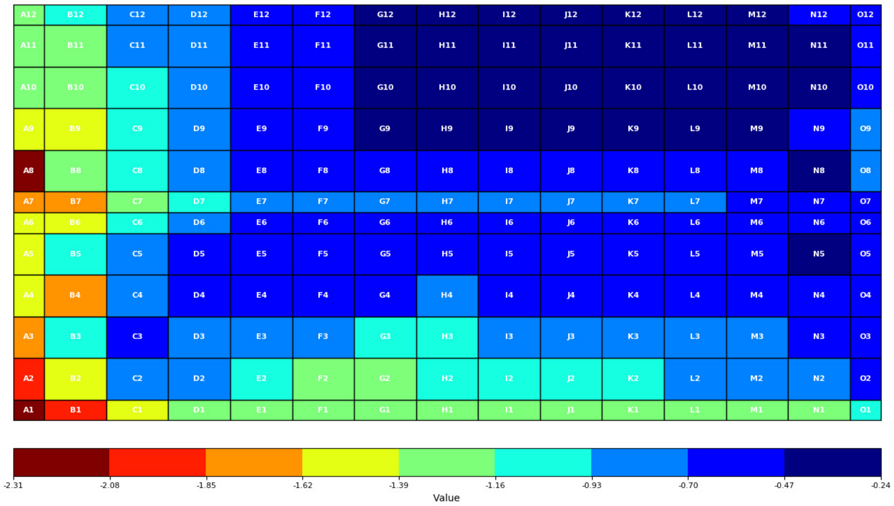

FIGURE 7 PLAN VIEW OF HOUSE ROOF SHOWING WIND PRESSURE DISTRIBUTION CFIG ON THE GROUP 4 HOUSE FOR WIND DIRECTION 225 ±20°

The VAWS program does not run a time history of wind pressures but increases the wind speed in increments to represent the increase in wind speed through a wind storm. Therefore locations of initiation and spread of failure through the structure is indicated by bands or sections of roof zones that fail at a range of increasing wind speeds.

Roof cladding failure causes loads to be redistributed to other cladding fasteners on neighbouring battens i.e. loads are redistributed along the direction parallel to the roof corrugations. Figure 8 shows that failure of cladding initiates on the windward roof slope near the gable end of the roof.

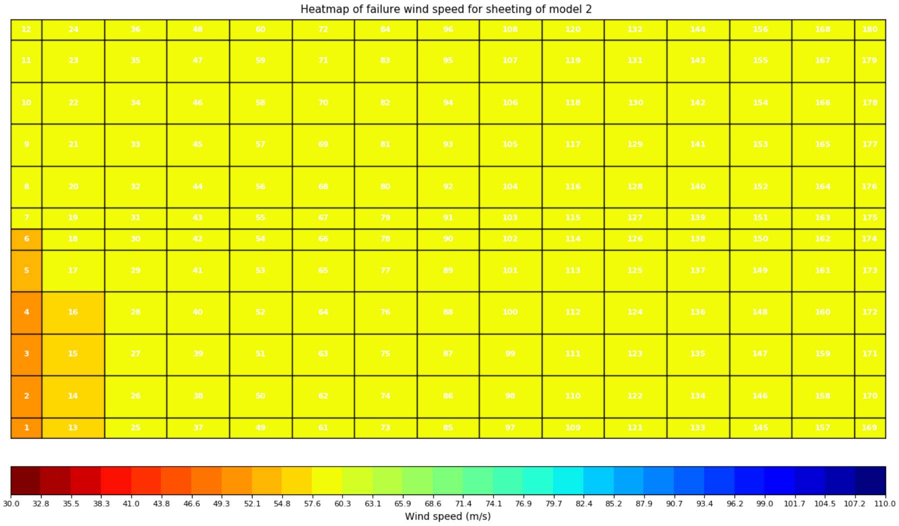

FIGURE 8 PLAN VIEW OF HOUSE ROOF SHOWING FAILURE WIND SPEEDS FOR ROOF CLADDING FOR A SINGLE MODEL RUN AT WIND DIRECTION 225 ±20°. NOTE THE LARGE SWATHE OF YELLOW INDICATING LARGE SCALE FAILURE AT ABOUT 57M/S CAUSED BY INTERNAL PRESSURISATION.

For this realisation, the batten to rafter connections are the first to fail, as shown in Figure 9. This is expected for this house type, where batten to rafter connections are generally the weakest link in the tie down chain. Batten to rafter failures cause loads to be redistributed to neighbouring intact batten to rafter connections along the same batten to the left and right. For a SW wind direction, failure initiates on the windward corner of the roof at the second batten in from the roof edge, which supports a larger tributary area than the edge batten. Failure then propagates along the batten towards the left with increasing wind speed increments.

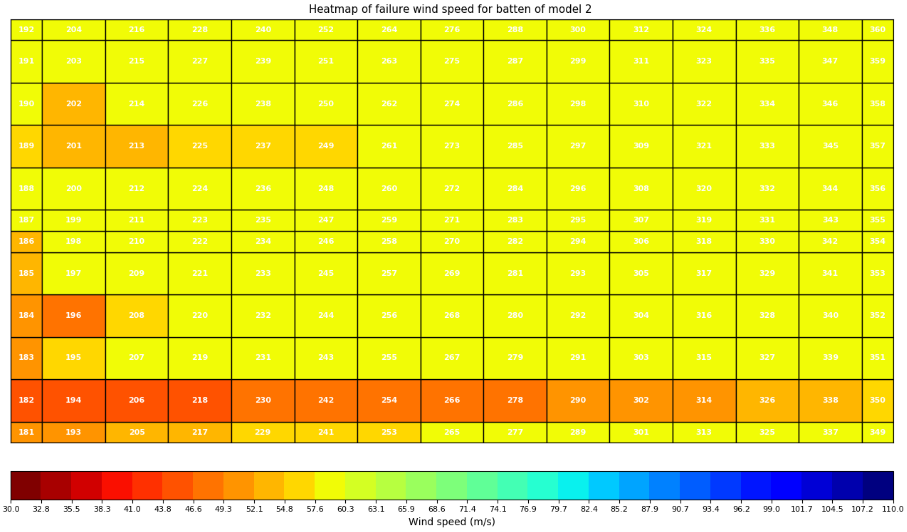

FIGURE 9 PLAN VIEW OF HOUSE ROOF SHOWING FAILURE WIND SPEEDS FOR BATTEN TO RAFTER CONNECTIONS FOR A SINGLE MODEL RUN AT WIND DIRECTION 225 ±20°. NOTE THAT LARGE SWATHE OF YELLOW INDICATING LARGE SCALE FAILURE AT ABOUT 57M/S CAUSED BY INTERNAL PRESSURISATION.

As described in Section 2 Load redistribution due to roof to wall connection failures is significantly more complex than cladding or batten failures. For this realisation, roof to wall connection failure initiates near the middle of the roof and is due to high loads being transferred here due to the failure of batten to rafter connections, at lower wind speeds, left of this location as shown in Figure 10.

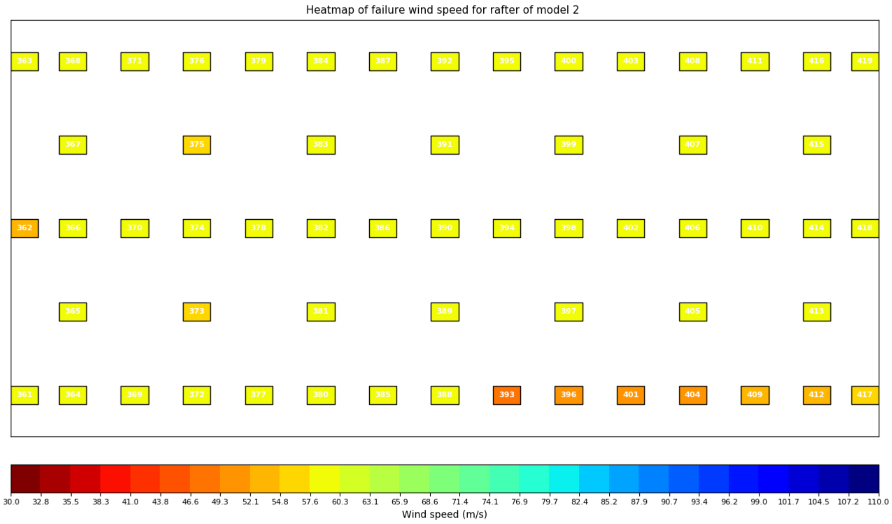

FIGURE 10 PLAN VIEW OF HOUSE ROOF SHOWING FAILURE WIND SPEEDS FOR ROOF TO WALL CONNECTIONS AND COLLAR TIES FOR A SINGLE MODEL RUN AT WIND DIRECTION 225 ±20°. NOTE THE NUMEROUS CONNECTIONS COLOURED YELLOW DENOTING FAILURE AT ABOUT 57M/S CAUSED BY INTERNAL PRESSURISATION.

For this realisation, internal pressurisation occurs due to debris impact on a door or window at about 57m/s, as shown in Figure 11. The sudden increase in loads immediately causes the failure of other roof to wall connections. Cladding fasteners and batten to rafter connections are also defined as failed for damage costing purposes, as they have been removed along with the rafters of the house.

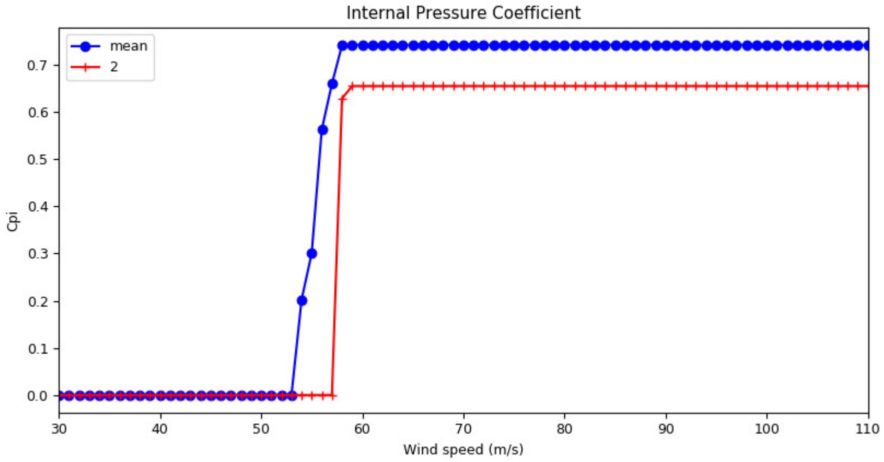

FIGURE 11 INTERNAL PRESSURE COEFFICIENTS FOR A SINGLE REALISATION (RED LINE) AS A FUNCTION OF WIND SPEED, INDICATING INTERNAL PRESSURISATION OCCURRING AT APPROX. 57M/S DUE TO DEBRIS IMPACT. THE BLUE LINE SHOWS THE AVERAGE CPI FROM MANY REALISATIONS OF THE MODELLED HOUSE.

Based on the repair cost and cost for full replacement, a damage index is calculated for each wind speed increment. As damage increases with increasing wind speed, the data points of damage index trace a vulnerability function for that house realisation, shown in Figure 12 .

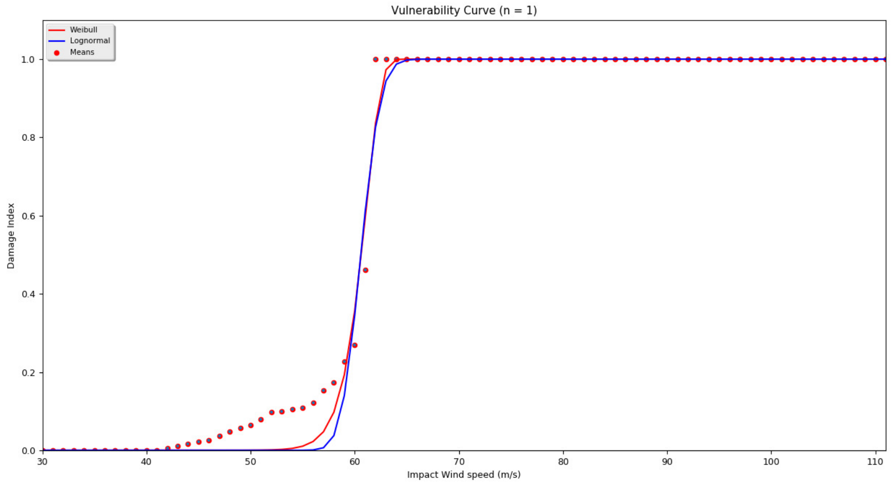

FIGURE 12 VULNERABILITY CURVE FOR A SINGLE REALISATION OF THE GROUP 4 HOUSE

## RESULTS FOR MULTIPLE WIND DIRECTIONS

The main purpose of VAWS is to determine vulnerability functions for a population of similar houses. Using a desktop computer the VAWS program can run hundreds of realisations of a house type within minutes to determine vulnerability functions for a population of houses. The results of 100 realisations of the Group 4 House type is presented in this section. Each realisation is assigned a wind direction, gust wind speed profile, external pressure coefficients and connection properties. Load redistribution and connection failure is calculated for each realisation as described in the previous section and internal pressurisation is determined based on the debris impact module.

As described in Section 0, the Damage Index (DI) based on cost of repair for each realisation is calculated at increasing wind speed increments. The results for each realisation together with mean DI as well as lognormal and Weibull fits of the data are shown in Figure 13. The wind speeds causing the onset of damage for most of the houses ranges between 37 to 53 m/s with a mean of 45m/s. And complete damage occurs from approx. 55 to 60m/s. Such onset and complete damage thresholds are similar to observations from post windstorm damage investigations conducted by the Cyclone Testing Station (Boughton, Falck et al. 2017).

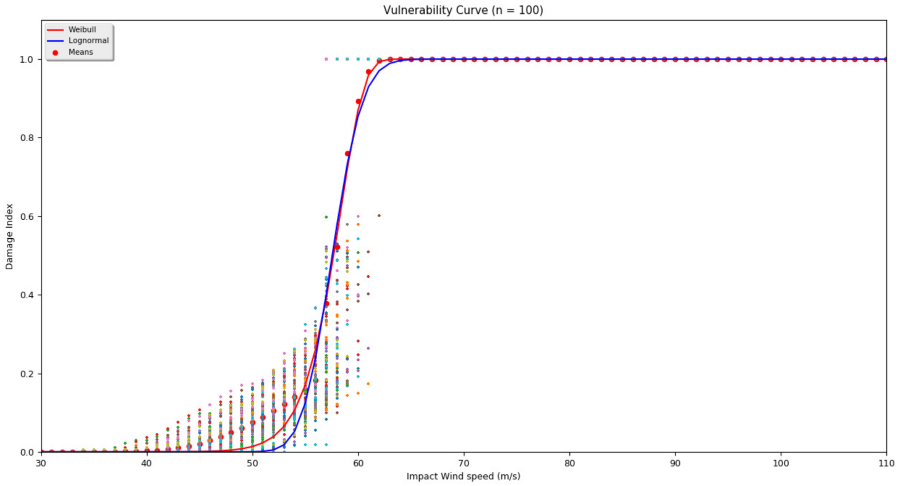

FIGURE 13 VULNERABILITY CURVES FOR 100 REALISATIONS OF THE GROUP 4 HOUSE

## Wind borne debris and internal pressures:

The trajectories and generation of windborne debris is modelled in detail through a process described in Wehner, Sandland et al. (2010). An example of debris landing locations, sources and the target house, for a single realisation at a single wind speed are shown in Figure 14.

The modelling of debris allows for cost of damaged wall cladding to be determined, more importantly breaches of the building envelope through broken windows trigger the internal pressurisation of the house. The overall percentage of breached houses in the population, approximately 25% in this case, is shown in Figure 15 along with the generation and exhaustion of debris with increasing wind speed.

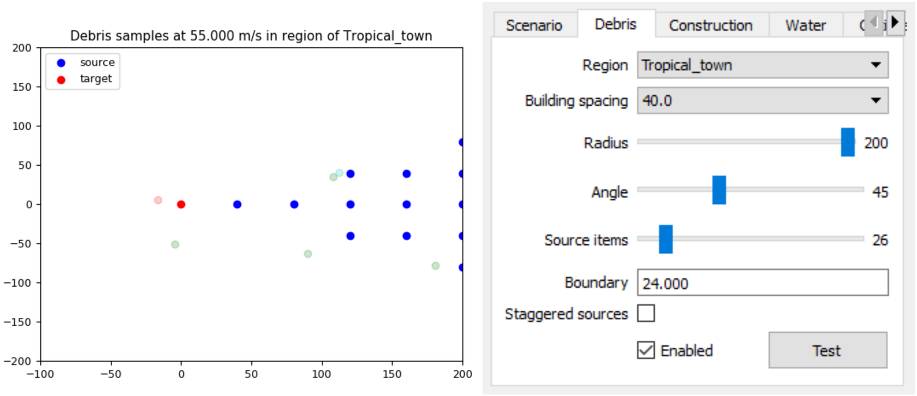

Region: Tropical_town

Building spacing: 40.0

Radius: 200

Angle: 45

Source items: 26

Boundary: 24.000

Staggered sources ☐

☑ Enabled

FIGURE 14 DEBRIS LANDING SITES, SOURCES AND TARGET HOUSE.

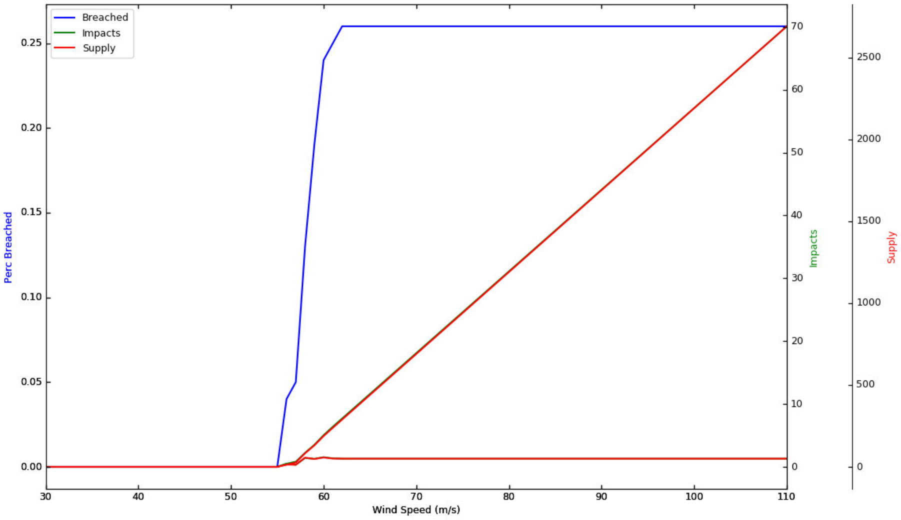

FIGURE 15 DEBRIS GENERATION, IMPACTS AND PERCENTAGE OF ENVELOP BREACHES AS A FUNCTION OF WIND SPEED. DEBRIS ITEM SUPPLY AND IMPACTS ARE SHOWN AS RED AND GREEN LINES RESPECTIVELY. PLOTS OF DEBRIS ITEM SUPPLY AND IMPACTS ARE PROVIDED FOR INDIVIDUAL WIND SPEEDS (LOWER LINES) AND ALSO AS A CUMULATIVE PLOT (INCLINED LINES).

## Validation

The VAWS software output is checked based on engineering judgement and observations from past damage surveys. Additionally, the Heuristic vulnerability curves by Wehner, Ginger et al. (2010) provide a starting point for validating the output of VAWS. Furthermore, structural behaviour is assessed using individual runs with a single wind direction and studying only one connection failure mode at a time. Results are compared with more detailed studies by Parackal (2018).

## Conclusions

This report has outlined the overall logic of the VAWS software package and presented a case study of highset Queensland House.

The VAWS program quantifies the vulnerability of a population of house types in Australia accounting for the variability in wind speed, external and internal pressures, debris impacts and connection strengths. Significantly advances in modelling lie in the modelling of debris impacts and in the load redistribution and progressive failures of connections in the structure.

The case study presented demonstrated load redistribution and spread of failure in the Group 4 house for increasing wind speeds. Although several simplifying assumptions are used to model failure efficiently, the modelled behaviour estimates a similar number of failed connection that would occur in a windstorm.

The simulation of 100 realisations of the Group 4 house allowed the fitting of vulnerability curves to the calculated damage index at each wind speed increment. Wind speeds of onset and complete failure of houses compare satisfactorily with observations from damage investigations.

# REFERENCES

Boughton, G., et al. (2017). Tropical Cyclone Debbie: Damage to buildings in the Whitsunday Region, Cyclone Testing Station, JCU, Report TR63.

GeoscienceAustralia (2019). VAWS User Manual v2.3.

Henderson, D. and B. Harper (2003). "Climate change and tropical cyclone impact on coastal communities' vulnerability." Queensland Government (Dept. of Natural Resources and Mines, and Dept. of Emergency Services), Brisbane, Australia.

JDHConsulting (2010). Contributions to development of a wind vulnerability model - final report 2009-2010, Report to Geoscience Australia.

Parackal, K. (2018). The Structural Response and Progressive Failure of Batten to Rafter Connections under Wind Loads. Cyclone Testing Station, James Cook University. PhD Thesis.

Standards Australia (2011). AS/NZS1170.2 - Structural design actions Part 2: Wind actions. Sydney, Australia.

Wehner, M., et al. (2010). Development of methods for assessing the vulnerability of Australian residential building stock to severe wind. IOP Conference Series: Earth and Environmental Science, IOP Publishing.

Wehner, M., et al. (2010). Modelling damage to residential buildings from wind-borne debris - Part 1, methodology. 14th Australasian Wind Engineering Society Workshop, Canberra, Australia.